

## **Modeling Of Superheated Steam Drying Of Wood Particles**

**K.H. Le<sup>†</sup>, T. T. H. Tran<sup>†\*</sup>, A. Kharaghani<sup>‡2</sup>, E. Tsotsas<sup>‡</sup>**

<sup>†</sup>School of Heat Engineering and Refrigeration, Hanoi University of Science and Technology, No. 01 Dai Co Viet Street, Hai Ba Trung, Hanoi, Vietnam

<sup>‡</sup>Thermal Process Engineering, Otto von Guericke University, PO 39106, Magdeburg, Germany

Corresponding Author Email: hang.tranthithu@hust.edu.vn

**ABSTRACT:** In this work, the superheated steam drying behavior of single wood particles at elevated temperature (i.e. 120°C, 140°C, 160°C and 180°C) are experimentally investigated by using a magnetic suspension balance system. To describe the experimental drying behavior, a coupled heat and mass transfer model of drying model is developed. The moisture diffusivity in the wood particles is determined from an inverse analysis, whereas other thermo-physical properties are measured. Two types of effective diffusivities, including moisture-dependent effective diffusivity and temperature-dependent effective diffusivity, are used to describe the moisture transport in the particles. This mathematical model is implemented and solved by using finite volume element method. Numerical results obtained with temperature-dependent effective diffusivity and moisture-dependent effective diffusivity are benchmarked by the experimental observations. It indicates that the drying behavior can accurately be described by the diffusion model using moisture-dependent effective diffusivity. Furthermore, a model-based sensitivity analysis is made to investigate the influence of drying conditions on the drying kinetics of the particles. The results obtained from the sensitivity analyses may help to optimize and customize dryer design and its operation in the future.

### INTRODUCTION

Wood is an important material which can be encountered in both daily life and industrial processes. To increase the durability and resistance from being destroyed by fungi, wood needs to be dehydrated to reach a safe moisture content level for storage and manufacturing. Recently, with the key advantages in energy saving and low carbon dioxide emission, superheated steam drying (SSD) with/without microwave or ultrasound assistance has been proved in many applications to be more appropriate compared to hot air drying (HAD) techniques [1–7]. The experimental studies have confirmed that the SSD technique can help to improve the quality of wood products compared to HAD [8-10].

Several theoretical studies of the heat and mass transfer inside porous media have been carried out to describe the SSD process of wood, a hygroscopic porous material. Most models were developed based on the phenomenological concept of effective water diffusivity. The main assumption used in diffusion models is that the gaseous pressure within the medium equals to the external pressure, or in other words, the advective vapor flow is negligible [11-13]. The impact of bound water, which is accumulated in nano-pore and in cellular cell, on the drying characteristics in diffusion models may be reproduced by introducing the moisture pseudo-diffusivity which is moisture-content or temperature dependent. The magnitude of this moisture diffusivity should decrease when the drying process progresses further. In this manner, the diffusion models can express the nature of dehydration process of hygroscopic porous materials where the dehydration of the bound water at low moisture content regime becomes more difficult compared to the removal of free water, located in macro and meso-pore, at high moisture content regime [13].

The effective water diffusivity has been determined for different varieties such as pine (*Pinus silvestris*) wood [14], softwood [15], sugar maple wood [4]. In the cited works up to here, the effective diffusivity has been considered as either a constant value or a function of temperature, the reduction of drying rate at the end of drying process due to a higher removal resistance of bound water, compared to free water, has not considered. Thus, this paper aims to express our effort to incorporate the impact of bound water on the magnitude of moisture diffusivity.

In this work, a comparative study is performed to evaluate two models of effective diffusivity, moisture-dependent effective diffusivity and temperature-dependent effective diffusivity, by benchmarking with experimental observation obtained by mean of a magnetic suspension balance system. Furthermore, the influence of drying conditions on the drying kinetics is investigated to pave a better way for dryer design and operation.

## MODEL DESCRIPTION

To develop the continuous model for SSD of single wood particles, several following assumptions are made.

- + The drying product is preheated up to the boiling temperature prior to drying, the surface condensation and evaporation periods are not accounted for.
- + Although porous wood is anatomically complex and heterogeneous, the transport properties of solid and fluid phases are averaged in a representative elementary volume by mean of volume averaging technique.

Heat and mass conservation equations

Mass conservation of water is written as the change of water concentration in the medium is caused by water diffusion flow

$$\frac{\partial \rho_0 X}{\partial t} + \nabla \cdot [-D_{eff} \nabla (\rho_0 X)] = 0 \quad (1)$$

where  $\rho_0 = \frac{M_s}{V}$  (kg dry solid/m<sup>3</sup>) is the apparent density of the dry porous medium,  $X = \frac{M_l}{M_s}$  (kg water/kg dry solid) is the moisture content of the solid.  $M_l$  and  $M_s$  (kg) are the mass of water and solid, respectively.  $D_{eff}$  (m<sup>2</sup>/s) is the effective diffusivity of moisture in the medium. To describe the reduction of magnitude of this moisture diffusivity when the moisture removes further, the moisture diffusivity is classically expressed by the Arrhenius equation

$$D_{eff} = D_0 \exp\left(-\frac{E_A}{RT}\right) \quad (2)$$

where  $D_0$  is the maximal diffusion coefficient,  $E_A$  is the activation energy for diffusion (J/mol),  $T$  is the absolute temperature (K),  $R$  is the universal gas constant, 8.314 J/(mol·K) [16]. The Arrhenius equations is often referred as temperature-dependent effective diffusivity (TDED).

Recently, Khan et al. [16] reported that the moisture diffusivity can be described as a function of moisture content, the so-called temperature-dependent effective diffusivity (MDED), as

$$D_{eff} = D_{ref} \left( \frac{1 + X_0}{1 + X} \frac{\rho_l (1 + X) + \rho_0 X}{\rho_l (1 + X_0) + \rho_0 X_0} \right)^2 \quad (3)$$

where  $D_{ref}$  (m<sup>2</sup>/s) is the reference diffusivity.

By minimization of the sum of square of difference between numerical and experimental moisture content evolutions over time, the reference diffusivity  $D_{ref}$  and maximal diffusivity  $D_0$  are determined by using an optimization procedure, i.e. *fminsearch* function in MATLAB software.

The energy conservation equation is written as the change of total energy due to the enthalpy flow of water diffusive flow and the conductive heat flow can be computed as

$$\begin{aligned} \frac{\partial}{\partial t} (h_s + h_l) - \nabla \cdot [h_l D_{eff} \nabla (\rho_0 X)] \\ - \nabla \cdot [\lambda_{eff} \nabla (T)] = 0 \end{aligned} \quad (4)$$

In Eq. 4,  $h_s$  and  $h_l$  (J/kg) denote the specific enthalpy of solid and liquid water, respectively. Assuming a constant value for the specific heat capacity, the specific enthalpy of the solid and of the liquid can respectively be calculated from temperature as

$$h_s = c_{p,s} (T - T_{ref}) \quad \text{and} \quad h_l = c_{p,l} (T - T_{ref}) \quad (5)$$

with the reference temperature  $T_{ref} = 0$  °C.  $\lambda_{eff}$  denotes the effective thermal conductivity of the porous grain.

Initial and boundary conditions

A wet spherical wood particle of radius  $r_p$  is surrounded by superheated steam flowing at a constant temperature of  $T_b$  and pressure of  $p_b$ . Initially, this porous grain is at uniform temperature  $T_0$  and moisture content  $X_0$  (kg water/kg dry solid). For the mass and heat transfer at the interface between the porous sample and the external bulk gas, the following boundary conditions are applied

$$j_w \cdot n = -\beta(\rho_{v,surf} - \rho_{v,b}) \quad (5)$$

$$j_e \cdot n = -\alpha(T_{g,b} - T) + (\Delta h_{evp} + c_{p,v}T)\beta(\rho_{v,surf} - \rho_{v,b}) \quad (6)$$

In Eqs. 5-6,  $n$  denotes the outward unit normal vector pointing out of sample surface,  $j_w$  and  $j_e$  are the water and energy fluxes transferred from the sample surface toward the bulk steam, respectively. The vapor density at the particle surface is calculated from the particle surface temperature and the bulk steam pressure. The heat transfer coefficient is calculated by using the modified Ranz - Marshall correlation proposed in Hager et al. [17].

$$Nu = 2 + 0.616 Re^{0.52} Pr^{\frac{1}{3}} \quad (7)$$

where  $Nu = \frac{\alpha d_p}{\lambda_v}$ ,  $Re = \frac{v_b d_p}{\nu_v}$  and  $Pr = \frac{c_{p,v} \mu_v}{\lambda_v}$  are the dimensionless Nusselt, Reynolds and Prandtl numbers, respectively. The thermo-physical properties of steam used in dimensionless number calculation are determined at  $T_b$  and  $p_{v,b}$ . The mass transfer coefficient is obtained by using an empirical correlation [18].

$$Sh = 0.144 + 0.579 Re^{0.5} Sc^{\frac{1}{3}} \quad (8)$$

where  $Sh = \frac{\beta d_p}{\delta_v}$  and  $Sc = \frac{\nu_v}{\delta_v}$  are the Sherwood and Schmidt numbers, respectively.  $\delta_v$  is the self-diffusivity of vapor, at atmospheric pressure it can be empirically computed as [14]

$$\delta_v = -1.057 \times 10^{-4} + 3.35 \times 10^{-7} T_b \quad (9)$$

## SUPERHEATED STEAM DRYING EXPERIMENTS

The superheated steam drying experiments of the single wood particles are performed in an apparatus shown in Fig. 1. Beechwood particles (provided by Holz-Allerlei GmbH, Germany) are consistent in shape and neither drilled nor waxed. Before commencing a drying experiment, the wood particles are moistened by soaking in liquid water at temperature 20 °C for 16 hours. This has led to an average initial moisture content of about  $0.752 \pm 0.023$  (kg water/kg dried solid). Other thermo-physical properties of wood material are measured directly in the frame of this work and has been published in our previous article where the detail measurement procedures are presented in detail. These parameters are summarized in Table 1.

This drying system is comprised of three main components: a micro-evaporator, a drying chamber and a magnetic suspension balance. The liquid water is pumped and injected into the micro-evaporator. In this evaporator, liquid evaporates, and the generated vapor is superheated. By using a controllable micro-pump and temperature controller, the mass flow rate and temperature of superheated steam can be adjusted. The superheated steam flows into drying chamber, interacts with wood particle and is released at the top of chamber. The mass evolution of particles is recorded by using a magnetic suspension balance (Rubotherm GmbH, Germany). The balance operates in a mass range up to 10 g with a measurement resolution of  $\pm 1$   $\mu$ g. The sample mass measurements are recorded by the Rubotherm system control software (RSCS), whereas temperature and pressure of the drying chamber are logged by using a data acquisition system (Omega, USA). The drying conditions and initial conditions used in drying experiments are listed in Table 2.

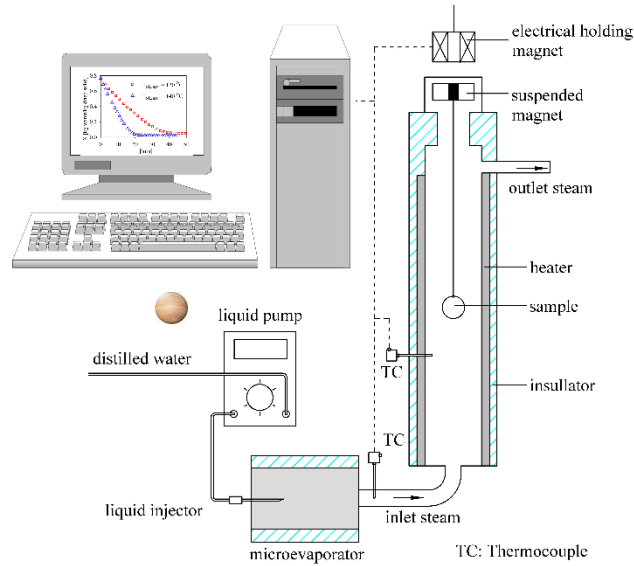


**Figure 1.** Schematic of the experimental setup used for drying of single wood particles.

**Table 1.** Thermo-physical properties of wood particles used in simulations.

Property	Value
Particle diameter $d_p$ , mm	$6.2 \pm 0.3$
Apparent solid density $\rho_b$ , kg/m <sup>3</sup>	743
Sorption isotherm $p_v/p_{v,sat}$ , -	$a_w = \begin{cases} 1 & \text{with } X > X_{irr} \\ \frac{X}{X_{irr}} \left( 2 - \frac{X}{X_{irr}} \right) & \text{with } X \leq X_{irr} \end{cases}$ $X_{irr} = 0.256 \text{ kg water/kg dry solid}$
Thermal conductivity $\lambda_{eff}$ , W/mK	$\lambda_{eff} = 0.138 + \frac{X \rho_b}{\rho_l} \lambda_l$
Specific heat capacity of dry solid $c_{p,s}$ , J/kgK	$770 \pm 3.6$

**Table 2.** The drying conditions and initial conditions used in simulation.

$T_b$ , °C	$v_b$ , m/s	$X_0$ , kg water/kg dry solid
120	0.015	0.758
140	0.015	0.765
160	0.015	0.729
180	0.015	0.756

RESULTS AND DISCUSSION

The wood particles before soaking, after soaking and after drying are presented in Fig. 2. It can be seen that the color and shape of the particles are optically prevented, it favors the application of SSD for wood material.



Figure 2. Wood particles before soaking, after soaking and after superheated steam drying.

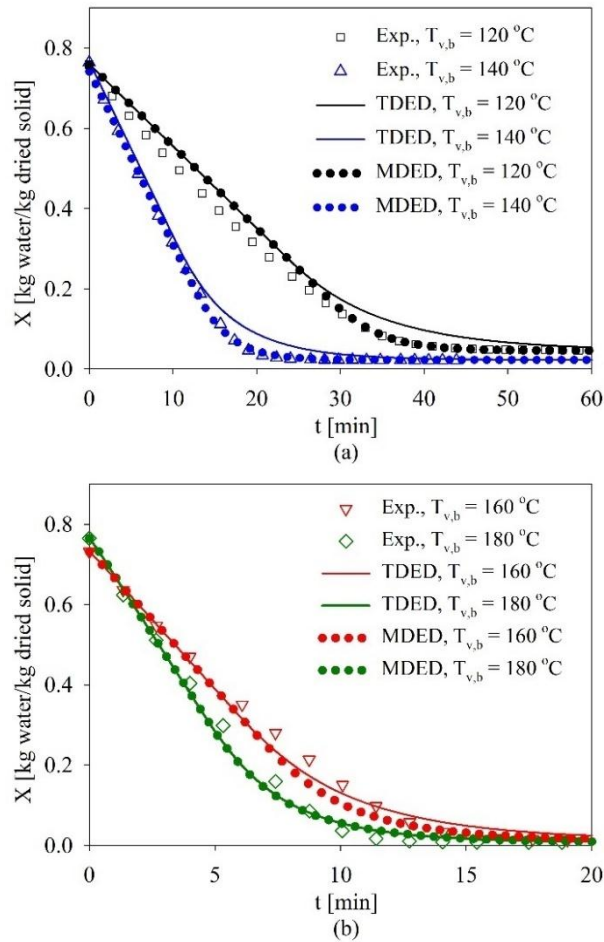
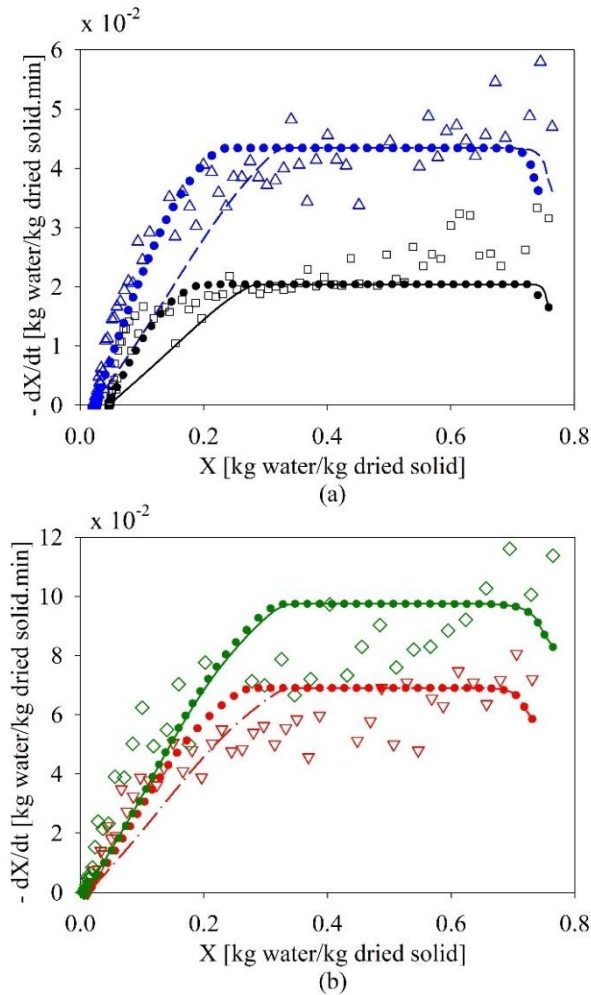


Figure 3. Experimental and numerical moisture content evolutions over time with different drying temperature: (a) 120 °C and 140 °C, (b) 160 °C and 180 °C.

The experimental moisture content evolutions over time are presented in Fig. 3. Based on the experimental data, the diffusivity of medium is calculated by running the optimization procedure. For MDED model, a reference diffusivity of  $7.13 \times 10^{-9} \text{ m}^2/\text{s}$  is obtained. For TDED model, the diffusivity varies in range from  $1.67 \times 10^{-9} \text{ m}^2/\text{s}$  to  $5.76 \times 10^{-9} \text{ m}^2/\text{s}$  when the drying temperature increases from 120 °C to 180 °C, respectively. Based on these data, maximal diffusivity of  $1.72 \times 10^{-5} \text{ m}^2/\text{s}$  and activation energy for diffusion 30138.25 J/mol are obtained. The range of diffusivity and activation energy values determined in this study closely agreed with the literature data [3,10-12]. The numerical observations obtained from the diffusion model with both MDED and TDED are also plotted in Fig. 3 together with experimental data. It can be seen; the experimental data can be fairly reflected by the diffusion model with both MDED and TDED models of moisture diffusivity. This result is in close agreement with the previous

studies.

A better agreement between experimental data and numerical observations obtained with MDED model is seen compared to TDED model. The moisture content generated with TDED model reduces slower than the experimental data and numerical data obtained with MDED model. Moisture content profile considering MDED agrees more closely, compared to experimental data, than that of TDED. At the end of drying process, when the falling drying rate period commences, the difference between moisture content evolutions obtained with MDED and TDED models becomes pronounced. It can be explained by the drying rate curve evolutions presented in Fig. 4. The numerical results obtained with MDED fits better to with experimental data therefore, it can be concluded that MDED is the more accurate approach for wood drying than TDED.



**Figure 4.** Experimental and numerical drying rate curves with different drying temperature: (a) 120 °C and 140 °C, (b) 160 °C and 180 °C.

Exemplarily, the internal moisture content and temperature distribution obtained with MDED and TDED with drying temperature of 160 °C are plotted for a time of  $t = 12$  min with an interval of 3 min are plotted in Fig. 5. As can be seen, during the constant drying rate period, the temperature generated numerically with MDED and TDED are identical, the mass transfer is solely controlled by the moisture diffusion. Since the diffusivity of TDED model at 160 °C is smaller than the reference diffusivity of MDED, the moisture at the surface in TDED simulation reduces faster than the MDED simulation (e.g. time of 2 minute and 4 minute). Therefore, the falling drying rate of TDED simulation commences sooner compared to MDED model. As a result, the moisture content of TDED simulation reduces slower compared to MDED model at the end of drying process as can be seen in Figs. 3 and 4. In light of these findings, it can be claimed that the moisture has more influence than the temperature in case of wood drying. In the next section, the influence of drying conditions on the drying kinetics is investigated by a MDED model-based sensitivity analyses.

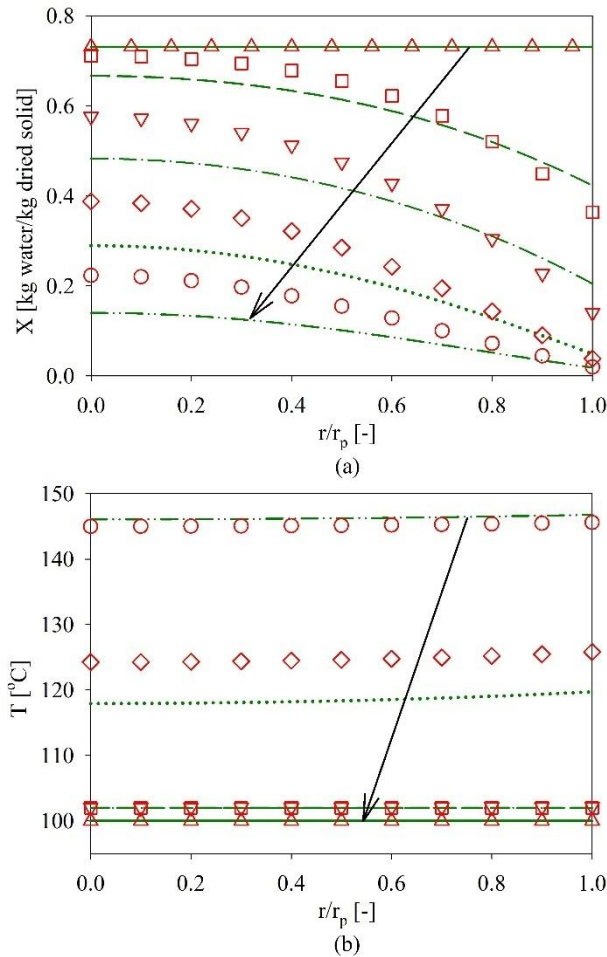


**Figure 5.** Simulated moisture content (a) and temperature (b) profiles of the wood particles obtained with MDED (line) and TDDED (symbol). The surface of the particle is located at  $r/r_p = 1$ . The profiles are plotted for a time period of  $t = 12$  min with an interval of 3 min. Parameters used in simulations are:  $T_{v,b} = 160$  °C,  $v_{v,b} = 0.015$  m/s and  $X_0 = 0.73$  kg water/kg dry solid.

The diffusion simulations are made with MDED model with different values of bulk steam velocity and of initial moisture content. The numerical evolutions of moisture content over time are presented in Figs. 6-8. As can be observed in Fig. 6, with the increase of bulk vapor velocity, the drying time reduces significantly. However, in high velocity range (i.e. 0.5 m/s and 1 m/s), the time saving is not remarkable. It implies that in high velocity range, the water removal is controlled by the internal mass transfer resistance and the increasing of velocity is not meaningful. Additionally, a low initial moisture content is only helps to shorten the constant drying rate period, the falling drying rate seemingly remains unchanged (c.f. Figs. 7 and 8).

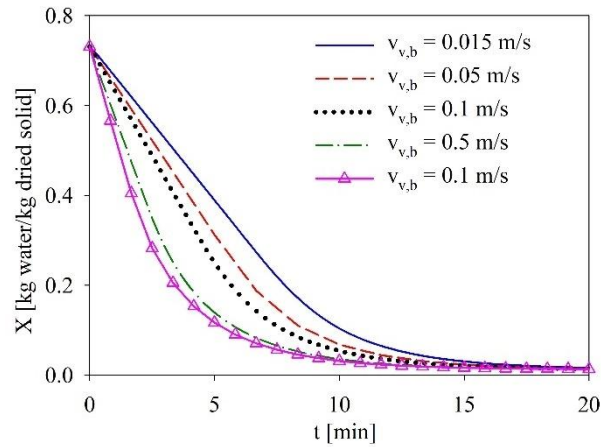


**Figure 6.** Simulated moisture content evolution of the wood particles obtained with MDED model with different bulk vapor velocity. Parameters used in simulations are:  $T_{v,b} = 160$  °C and  $X_0 = 0.73$  kg water/kg dry solid.

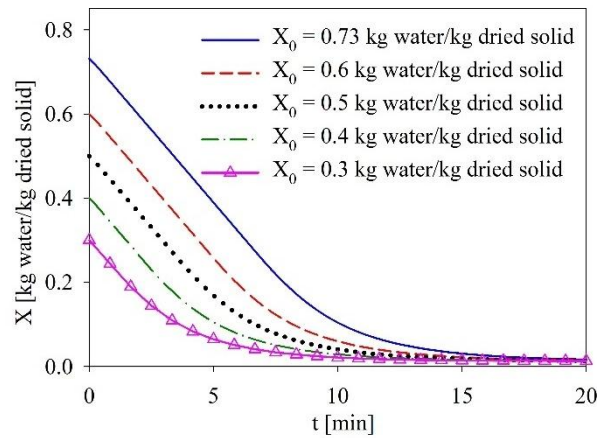


**Figure 7.** Simulated moisture content evolution of the wood particles obtained with MDED model with different initial moisture content. Parameters used in simulations are:  $T_{v,b} = 160$  °C and  $v_{v,b} = 0.015$  m/s.

## CONCLUSIONS

In this work, a diffusion model is developed to describe the heat and mass transfer inside single wood particles subjected to superheated steam drying. The model is validated successfully by benchmarking against experimental data obtained by mean of magnetic suspension balance system. By analysis the experimental and numerical data, several conclusions can be drawn.

- The superheated steam drying can be applied for wood material since the color of the particles is prevented.
- The superheated steam drying of wood particles can be describe by diffusion model. The moisture-dependent effective diffusivity is more appropriate to be used in diffusion model of wood particle superheated steam drying.
- The impact of vapor velocity on drying kinetic is significant in low value range of velocity, it become insignificant in high value range.
- With initial moisture content values higher than the irreducible moisture content, the initial moisture content influences only on the constant drying period.



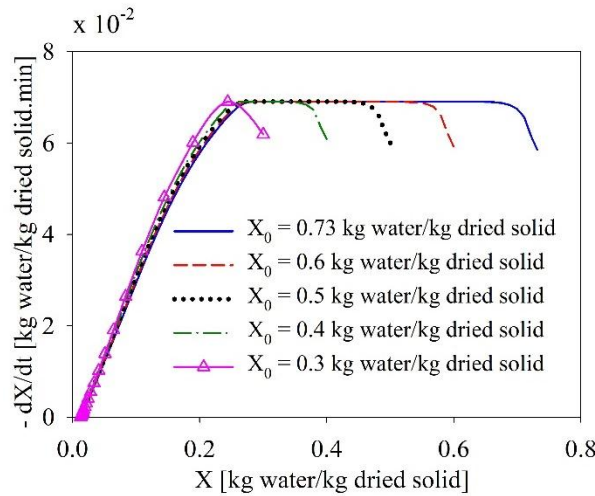


**Figure 8.** Simulated drying rate curve of the wood particles obtained with MDED model with different initial moisture content. Parameters used in simulations are:  $T_{v,b} = 160$  °C and  $v_{v,b} = 0.015$  m/s.

In the future, the diffusion model can be extended to describe fully superheated steam drying process, i.e. including condensation period. The inversed method used in this work to determine moisture diffusivity can be applied to estimate moisture diffusivity of other porous products.

#### ACKNOWLEDGEMENTS

This research is funded by the Hanoi University of Science and Technology (HUST) under project number T2018-TT-004.

#### NOMENCLATURE

- $c_p$  specific heat, J/(kg·K)
- $d$  diameter, m
- $D_{eff}$  effective diffusivity, m<sup>2</sup>/s
- $E_a$  activation energy of diffusion, J/mol
- $h$  specific enthalpy, J/kg
- $T$  temperature, °C/K
- $X$  moisture content, kg water/kg dried solid
- $\alpha$  heat transfer coefficient, W/(m<sup>2</sup>·K)
- $\beta$  mass transfer coefficient, m<sup>2</sup>/s
- $\lambda$  thermal conductivity, W/mK
- $\rho_0$  apparent density, kg dry solid/m<sup>3</sup>
- $\delta$  self diffusivity, m<sup>2</sup>/s
- $\nu$  kinematic viscosity, m<sup>2</sup>/s

#### Subscripts

- l liquid
- s solid
- surf surface

sat saturation

v vapor

ref reference

## REFERENCES

- [1] J. Ratnasingam, R. Grohmann. "Superheated steam application to optimize the kiln drying of rubberwood (*Hevea brasiliensis*)". *European Journal of Wood and Wood Products*, Vol. 73, no. 3, pp.407–409. 2015.
- [2] A.L. Redman, "Evaluation of super-heated steam vacuum drying viability and development of a predictive drying model for four Australian hardwood species". *Forest & Wood Products Australia Limited: Melbourne*, 2011.
- [3] S. Senthilananthan. "The Role Of The Audit Committee In NSW Local Council And Governance". *Advances In Industrial Engineering And Management*, vol. 2, no. 8, 75-81, 2019.
- [4] M. Defo, Y. Fortin, A. Cloutier, "Modeling superheated steam vacuum drying of wood". *Drying Technology*, vol. 22, no. 10, pp.2231–2253. 2004.
- [5] S. Pang, H. Pearson, "Experimental investigation and practical application of superheated steam drying technology for softwood Timber". *Drying Technology*, vol. 22, no. 9, pp.2079–2094. 2004.
- [6] B.M. Faraj and F.W. Ahmed, "On The Matlab Technique By Using Laplace Transform For Solving Second Order Ode With Initial Conditions Exactly", *Matrix Science Mathematic*, vol. 3, no. 2, pp.8-10, 2019.
- [7] R. Yamsaengsung, S. Tabtiang, "Hybrid drying of rubberwood using superheated steam and hot air in a pilot-scale". *Drying Technology*, vol. 29, no. 10, pp.1170–1178. 2011.
- [8] Y. Bao, Y. Zhou, "Comparative study of moisture absorption and dimensional stability of Chinese cedar wood with conventional drying and superheated steam drying". *Drying Technology*, vol. 35, no. 7, pp.860–866. 2016.
- [9] A.H. Khan, M.S. Islam. "A PCTTRAN-Based Investigation On The Effect Of Inadvertent Control Rod Withdrawal On The Thermal-Hydraulic Parameters Of A Vver-1200 Nuclear Power Reactor", *Acta Mechanica Malaysia*, vol.2, no. 2, pp. 32-38, 2019.
- [10] S. Yi, B. Zhang, J. Chang, C. Du, "Drying characteristics of wood under vacuum-superheated steam". *Forestry Studies in China*, vol. 6, no. 2, pp.41–45. 2004.
- [11] P. Perré, "The proper use of mass diffusion equations in drying modeling: Introducing the drying intensity number". *Drying Technology*, vol. 33, no. 15-16, pp.1949–1962. 2015.
- [12] K.S. Shazwan, R. Shahari, C.N.A. Che Amri and N.S. Mohd Tajuddin. "Figs (*Ficus Carica* L.): Cultivation Method And Production Based In Malaysia", *Engineering Heritage Journal*, vol. 3, no. 2, pp. 6-8, 2019.
- [13] K.H. Le, N. Hampel, A. Kharaghani, A. Bück, E. Tsotsas, "Superheated steam drying of single wood particles: A characteristic drying curve model deduced from continuum model simulations and assessed by experiments". *Drying Technology*, vol. 35, no. 15, pp.1866-1881. 2018.
- [14] R. Adamski, Z. Pakowski, "Identification of effective diffusivities in anisotropic material of pine wood during drying with superheated steam". *Drying Technology*, vol. 31, no. 3, pp.264–268. 2013.
- [15] P. Perre, M. Moser, M. Martin, "Advances in transport phenomena during convective drying with superheated steam and moist air". *International Journal of Heat and Mass Transfer*, vol. 36, no. 11, pp.2725–2746. 1993.
- [16] M.I.H. Khan, C. Kumar, M.U.H. Joardder, M.A. Karim, "Determination of appropriate effective diffusivity for different food materials". *Drying Technology*, vol. 35, no. 3, pp.335–346. 2016.
- [17] J. Hager, M. Hermansson, R. Wimmerstedt, "Modelling steam drying of a single porous ceramic sphere: Experiments and simulations". *Chemical Engineering Science*, vol. 52, no. 8, pp.1253–1264. 1997.

- [18] M.W. Woo, D. Stokie, W.L. Choo, S. Bhattacharya, "Master curve behaviour in superheated steam drying of small porous particles". *Applied Thermal Engineering*, vol. 52, no. 2, pp.460–467. 2013.